Magnetic vortex dynamics in a two-dimensional square lattice of ferromagnetic nanodisks

Junya Shibata[1,2] and Yoshichika Otani[1,2]
[1]*Frontier Research System (FRS), The Institute of Physical and Chemical Research (RIKEN), 2-1 Hirosawa, Wako, Saitama 351-0198, Japan*
[2]*Core Research for Evolutional Science and Technology (CREST), Japan Science and Technology Corporation (JST), Japan*
(Received 23 February 2004; published 13 July 2004)

The dynamics of magnetostatically coupled vortices in ferromagnetic two-dimensional (2D) nanodisk arrays is theoretically investigated using the rigid vortex model and Thiele's equation whereby the circular motion with the lowest energy for each vortex core is described. We present here dispersion relations and density of states for eigenfrequencies of coherently rotating vortices with ordered core polarizations. This behavior is analogous to the lattice vibration of a 2D molecule bound with a dipolar interaction.

DOI: 10.1103/PhysRevB.70.012404 PACS number(s): 75.40.Gb, 75.25.+z, 75.75.+a

Experimental observations by means of magnetic force microscopy[1] and spin-polarized tunneling microscopy[2] have recently revealed the presence of the out-of-plane magnetization component in the vortex core as calculated by Feldtkeller *et al.* in the 1960s.[3–5] An array of magnetic vortices in ferromagnetic nanodisks have then drawn renewed attention because of their potentialities as novel patterned recording media as well as a model system for research on nanomagnetism.[6–11] The static properties of magnetic vortices have been intensively studied so far. The general research objective on magnetic vortices has now gradually shifted towards dynamic properties.

Theoretical analyses on the dynamics of the off-centered vortex, for example, have shown the circular motion around the disk center where the rotational direction depends on the sign of the core polarization.[12,13] Such a circular motion has been recently observed by means of time-resolved Kerr microscopy.[14] In our previous work,[15] we have theoretically demonstrated that the magnetostatically coupled two vortices coherently rotate around the disk centers with eigenfrequencies given by the combinations of vortex core polarizations. We have also drawn an analogy between this vortex system and a van der Waals diatomic molecule.

There are millions of magnetostatically coupled magnetic nanodisks in a fabricated array. In analogy with the coupled two-vortex system, the many-vortex system should exhibit collective rotational motions of vortices dependent on the combination of vortex core polarizations in a two-dimensional (2D) lattice bound by dipolar interactions. In this study we thus investigate the dynamics of magnetostatically coupled vortices in the $N \times N$ vortex lattice.

For this analysis, the rigid vortex model[16] is employed to describe the vortex configuration, and Thiele's equation[17,18] is used to formulate the collective motion of vortices. It should be noted that this rigid vortex model is considered effective for the qualitative understanding for the case of small enough vortex displacements.[12] We calculate eigenfrequencies for the magnetostatically coupled vortex lattice with various combinations of vortex core polarizations. We show that the vortex lattice with ordered core polarizations exhibits the collective circular motion of vortices that satisfies the dispersion relations of eigenfrequencies in reciprocal space. Furthermore, we can design a density of states for eigenfrequencies by choosing combinations of vortex core polarizations.

Let us calculate the interaction energy of magnetostatically coupled vortices. We consider here a square lattice system with a nanodisk array as shown in Fig. 1. The separating distance between each disk center is defined as $D \equiv dR$, where R is the disk radius and d is the nondimensional separating distance.

When each vortex core is shifted from its disk center, magnetic charges emerge on the side surface of the disk and each vortex then magnetostatically interacts with each other. Here, we assume the vortex displacement is much smaller than the disk radius. Using the rigid vortex model[16] and a calculation method similar to that of Ref. 15, the magnetostatic energy can be expressed as a function of the nondimensional vortex displacement from each disk center, $\mathbf{x}_{i,j} = x_{i,j}\mathbf{e}_x + y_{i,j}\mathbf{e}_y$:

$$W_{i,j}^{\mathrm{int}} = C_{i,j}(I_{i,j}^{x} x_{i,j} + I_{i,j}^{y} y_{i,j}) + \mathcal{O}(|\mathbf{x}_{i,j}|^3), \tag{1}$$

where $C_{i,j}$ is the (i,j)th chirality, which refers the counterclockwise ($C_{i,j}=1$) or the clockwise ($C_{i,j}=-1$) rotational di-

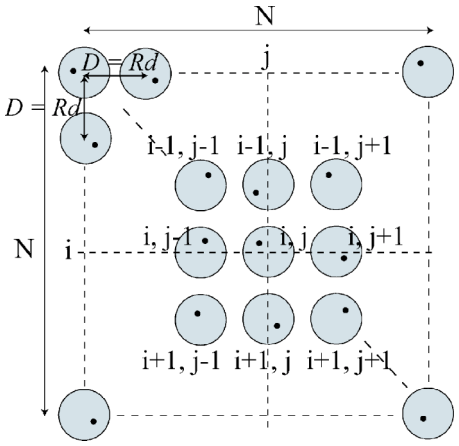

FIG. 1. Schematic illustration of a square $N \times N$ nanodisk array. Black dots represent off-centered vortices.

rection of the magnetization in the disk plane, and

$$I^x_{i,j} = \delta_1(d,0)\sum_{l=\pm1} C_{i,j+l}x_{i,j+l} + \delta_2(d,0)\sum_{k=\pm1} C_{i+k,j}x_{i+k,j} + \delta_1(d,d)\sum_{k,l=\pm1} C_{i+k,j+l}x_{i+k,j+l} + \delta_3(d,d)\sum_{k,l=\pm1}(kl)C_{i+k,j+l}y_{i+k,j+l}, \tag{2a}$$

$$I^y_{ij} = \delta_1(d,0)\sum_{k=\pm1} C_{i+k,j}y_{i+k,j} + \delta_2(d,0)\sum_{l=\pm1} C_{i,j+l}y_{i,j+l} + \delta_1(d,d)\sum_{k,l=\pm1} C_{i+k,j+l}y_{i+k,j+l} + \delta_3(d,d)\sum_{k,l=\pm1}(kl)C_{i+k,j+l}x_{i+k,j+l}, \tag{2b}$$

$$\delta_1(a,b) = \frac{\mu_0 M_s^2 R^3}{8\pi}\int \frac{dz_1 dz_2 d\phi_1 d\phi_2 \sin\phi_1 \sin\phi_2}{K(a,b,\phi_1,z_1,\phi_2,z_2)}, \tag{3a}$$

$$\delta_2(d,0) = \frac{\mu_0 M_s^2 R^3}{8\pi}\int \frac{dz_1 dz_2 d\phi_1 d\phi_2 \cos\phi_1 \cos\phi_2}{K(d,0,\phi_1,z_1,\phi_2,z_2)}, \tag{3b}$$

$$\delta_3(d,d) = \frac{\mu_0 M_s^2 R^3}{8\pi}\int \frac{dz_1 dz_2 d\phi_1 d\phi_2 \sin\phi_1 \cos\phi_2}{K(d,d,\phi_1,z_1,\phi_2,z_2)}, \tag{3c}$$

$$K(a,b,\phi_1,z_1,\phi_2,z_2) = [a^2+b^2+2a(\cos\phi_2-\cos\phi_1) + 2b(\sin\phi_2-\sin\phi_1)+2 - 2\cos(\phi_2-\phi_1)+(z_2-z_1)^2]^{1/2}, \tag{4}$$

where M_s is the saturation magnetization and $K(a,b,\phi_1,z_1,\phi_2,z_2)$ is a demagnetizing function. The integration of Eq. (3) runs from 0 to $g=L/R$ in z_1,z_2 and from 0 to 2π in ϕ_1,ϕ_2, where L is the disk thickness. Note that the x axis is defined as the horizontal direction while the y axis is the vertical direction; polar angles ϕ_1 and ϕ_2 are measured at each disk center from the x axis. Since the core radius of the vortex is small enough compared to the disk radius R, the magnetostatic interactions between the magnetic charges distributed on the top and bottom surfaces of neighbor disks are negligible. The total energy of off-centered vortices in the square lattice system is given by adding the interaction energy in Eq. (1) to the energy in Ref. 16,

$$W(\{\mathbf{x}\}) = \sum_{i,j=1}^{N} W_{i,j}, \quad W_{i,j} = W_{es}(|\mathbf{x}_{i,j}|) + W^{int}_{i,j}. \tag{5}$$

Here, $W_{es}(|\mathbf{x}_{i,j}|)=\xi|\mathbf{x}_{i,j}|^2/2+\mathcal{O}(|\mathbf{x}_{i,j}|^4)$ is the sum of the exchange and magnetostatic energies of the single off-centered vortex. In the equation, $\xi=\mu_0 M_s^2 V[F_1(g)-(R_E/R)^2]$ with $F_1(g)=\int_0^\infty dk\, f(kg)J_1^2(k)/k$, $f(x)=1-(1-e^{-x})/x$, V is the volume of the disk, $R_E\equiv\sqrt{A/\mu_0}M_s^{-1}$ is the exchange length with the exchange stiffness constant A, and $J_1(x)$ is the Bessel function of first order.

The formulation of the dynamics of vortices is based on Thiele's equation.[17,18] This equation is described by collective degrees of freedom of magnetic domains derived from the Landau-Lifshitz-Gilbert equation. Conditions for applying Thiele's equation are the constant saturation magnetization M_s and the vortex core displacement without distortion. In the case of a magnetic vortex, these collective degrees of freedom are the core position of the vortex. Here we consider the time-dependent nondimensional displacement $\boldsymbol{x}_{i,j}(t)$. Using $\boldsymbol{x}_{i,j}(t)$, the equation of motion of the vortex center can be written as

$$\boldsymbol{G}_{i,j}\times\frac{d\boldsymbol{x}_{i,j}(t)}{dt} = \frac{1}{R^2}\frac{\partial W(\{\boldsymbol{x}(t)\})}{\partial \boldsymbol{x}_{i,j}(t)}, \tag{6}$$

where $\boldsymbol{G}_{i,j}$ is the gyrovector given by $\mathbf{G}_{i,j}=-2\pi p_{i,j}L\mu_0 M_s\mathbf{e}_z/\gamma$, where γ is the gyromagnetic ratio, and $p_{i,j}$ is the (i,j)th polarization, which refers to the magnetization direction of the vortex core. The up or down magnetization of the vortex core corresponds to $p_{i,j}=1$ or -1, respectively. In this calculation, we ignore the damping. Equation (6) thus yields concretely a set of following equations:

$$\frac{dx_{i,j}(t)}{dt} = -p_{i,j}\omega_0(y_{i,j}+C_{i,j}I^y_{i,j}/\xi), \tag{7a}$$

$$\frac{dy_{i,j}(t)}{dt} = p_{i,j}\omega_0(x_{i,j}+C_{i,j}I^x_{i,j}/\xi), \tag{7b}$$

where $\omega_0=\gamma M_s[F_1(g)-(R_E/R)^2]/2$ is the characteristic frequency of the circulating single vortex. In the absence of interactions $I^x_{i,j}=I^y_{i,j}=0$, all vortices rotate independently around each disk center with eigenfrequency ω_0. Furthermore, the vortex core polarization determines the rotational direction of vortex. When polarization $p_{i,j}=1$ (-1), the vortex rotates in the counterclockwise (clockwise) direction. Note that the chirality $C_{i,j}$ of the vortex does not influence the dynamics of the vortex. On the other hand, in the presence of interactions $I^x_{i,j}$, $I^y_{i,j}$, the degeneracy of eigenfrequencies is removed, and various eigenfrequencies appear for the rotational motions of vortices in accordance with various combinations of polarizations of vortices.

We now consider three types of orderly polarized vortex lattices labeled types I, II, and III, corresponding to the combinations of polarizations of vortices, $p_{i,j}=1$, $p_{i,j}=(-1)^{i+j}$, and $p_{i,j}=(-1)^{i+1}$ as depicted in Fig. 2. Assuming the infinite lattice system, we can analytically calculate the eigenfrequencies from the Fourier transform of Eqs. (7). The obtained eigenfrequencies are

$$[\omega^{I}(k_x,k_y)/\omega_0]^2 = (1+a_1+a_3)(1+a_2+a_3)-a_4^2, \tag{8a}$$

$$[\omega^{II}_{\pm}(k_x,k_y)/\omega_0]^2 = 1+a_3(2+a_3)-a_1a_2 - a_4^2 \pm \sqrt{(1+a_3)^2(a_1-a_2)^2+4a_1a_2a_4^2}, \tag{8b}$$

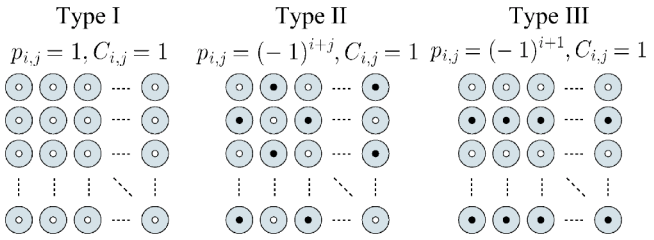

FIG. 2. Schematic diagram of vortices for various combinations of polarizations $p_{i,j}$. White dots and black dots represent vortex core polarizations, $p=+1$ and $p=-1$, respectively.

$$[\omega_{\pm}^{\mathrm{III}}(k_x,k_y)/\omega_0]^2 = (1+a_5)(1+a_6)+a_4^2-a_7a_8 \pm \sqrt{[a_7(1+a_5)-a_8(1+a_6)]^2+4(1+a_5)(1+a_6)a_4^2}, \tag{8c}$$

where (k_x,k_y) is the wave vector in the reciprocal-lattice space of the array, and

$$a_1 = 2(\alpha_1 \cos k_x d + \alpha_2 \cos k_y d), \tag{9a}$$

$$a_2 = 2(\alpha_1 \cos k_y d + \alpha_2 \cos k_x d), \tag{9b}$$

$$a_3 = 4\alpha_3 \cos k_x d \cos k_y d, \tag{9c}$$

$$a_4 = -4\alpha_4 \sin k_x d \sin k_y d, \tag{9d}$$

$$a_5 = 2\alpha_1 \cos k_x d, \tag{9e}$$

$$a_6 = 2\alpha_2 \cos k_x d, \tag{9f}$$

$$a_7 = 2\alpha_1 \cos k_y d + a_3, \tag{9g}$$

$$a_8 = 2\alpha_2 \cos k_y d + a_3, \tag{9h}$$

where $\alpha_1 \equiv \delta_1(d,0)/\xi$, $\alpha_2 \equiv \delta_2(d,0)/\xi$, $\alpha_3 \equiv \delta_1(d,d)/\xi$, and $\alpha_4 \equiv \delta_3(d,d)/\xi$.

Here, we take Permalloy as the computational material with the saturation magnetization $M_s = 8.60\times10^5$ A/m, the exchange stiffness constant $A = 1.3\times10^{-11}$ J/m, the gyromagnetic constant $\gamma = 2.2\times10^5$ m/A s, the disk radius $R = 100$ nm, the disk thickness $L = 20$ nm, and the separating distance $D = 240$ nm. Figures 3(a), 3(b), and 3(c) show calculated dispersion relations of eigenfrequencies for types I, II, and III, respectively. In Fig. 3(a) for type I, the dispersion curve corresponds well to that of the lattice vibration for monatomic square lattice system. However, since the off-centered vortex motion is limited to the rotational motion, there is only the single branch with nonzero eigenfrequency at $\Gamma(\mathbf{k}=0)$ in the reciprocal-lattice space. In Figs. 3(b) and 3(c) for types II and III, there are two branches represented by solid and dashed lines, corresponding, respectively, to the polarization $p=1$ or -1. These dispersion curves also show nonzero mode eigenfrequencies at Γ. In the case of minimum (maximum) eigenfrequencies for all the types, off-centered vortices rotate in (out of) phase. Note that type I takes the minimum in the difference between maximum and minimum eigenfrequencies, whereas type II takes the maximum in the difference. This can be understood as follows: since the rotational direction of the off-centered vortex is decided by the

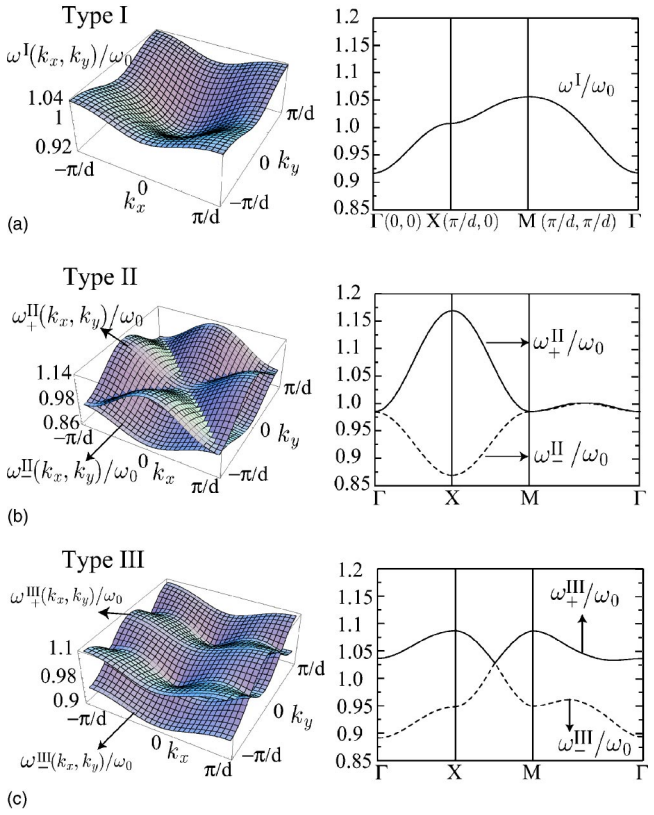

FIG. 3. (Color online) Dispersion relations of eigenfrequencies for types I, II, and III.

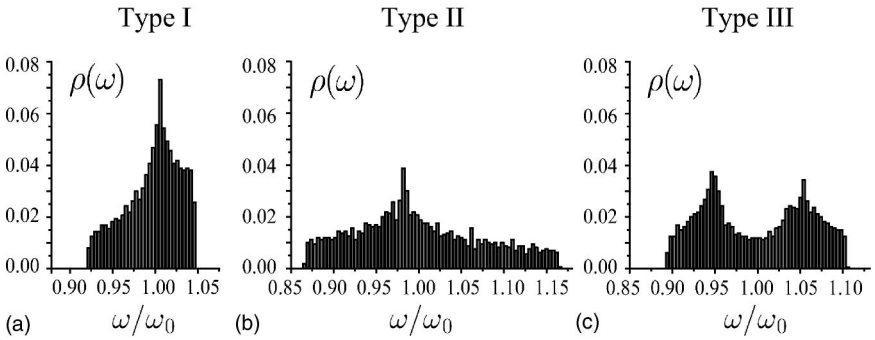

FIG. 4. Density of states for different combinations of polarizations of vortices: (a) $p_{i,j}=1$, (b) $p_{i,j}=(-1)^{i+j}$, and (c) $p_{i,j}=(-1)^{i+1}$.

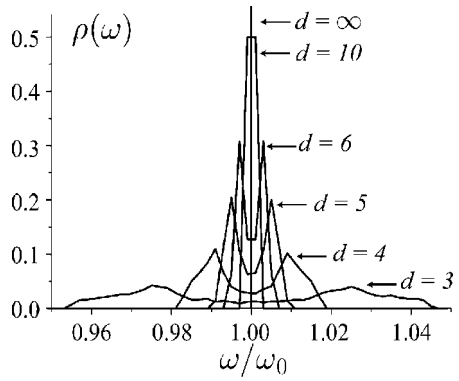

FIG. 5. Dependence on the nondimensional separating distance $d=D/R$ of the density of states for type III.

sign of core polarization, all vortices in type I rotate in the same direction. On the other hand, in type II, all the neighboring vortices rotate in opposite directions. This difference is important in determining the dipolar coupling of off-centered vortices. As explained in Ref. 15, the averaged energy of vortices with ferromagnetically polarized cores ($p_1=p_2=1$) is smaller than that of vortices with antiferromagnetically polarized cores ($p_1=-p_2=1$).[15] This causes significant difference in the eigenfrequencies.

To obtain the density of states for the eigenfrequencies, we here numerically evaluate eigenfrequencies of Eq. (7) for vortices with various types of core polarizations. Setting $\boldsymbol{x}_{i,j}(t)=\exp(-i\omega t)\boldsymbol{x}_{i,j}$ in Eq. (7) yields the eigenfunction for eigenfrequency. We then perform the numerical diagonalization for this eigenfunction to obtain eigenfrequencies for various combinations of polarizations of vortices; $p_{i,j}=1$, $p_{i,j}=(-1)^{i+j}$, and $p_{i,j}=(-1)^{i+1}$. Here we take $N\times N$ disk arrays with $N=40$ for calculation.

Figure 4 shows density of states (DOS) for eigenfrequencies, $\rho(\omega)=\Sigma_{l=1}^{1600}\,\delta(\omega-\omega_l)/N^2$, as a function of normalized frequency ω/ω_0 for vortices with various combinations of core polarizations. The DOS exhibits a single peak for types I and II and double peaks for type III. These peaks correspond to the local minima of the dispersion relations in Fig. 3. For example, the peak in type I at $\omega/\omega_0=1$ [Fig. 4(a)] corresponds to the local minimum at $X(\pi/d,0)$ in Fig. 3(a). For type III, polarizations along the x direction correspond to that of type I (ferromagnetic polarizations), while polarizations along the y direction correspond to type II (antiferromagnetic polarization). Therefore, double peaks in type III are observed due to the superposed effects of types I and II.

Finally, Fig. 5 shows the DOS for type III as a function of the nondimensional separating distance $d=D/R$. When the separating distance is increased, the double peaks gradually approach to the center. Note that the difference in frequency between double peaks varies proportional to the minus sixth power of the separating distance, characteristic of van der Walls bonding.

We have investigated theoretically the dynamics of vortices in a square lattice system with various combinations of vortex core polarizations in the lattice. The vortex core polarizations play an important role in determining the rotational dynamics of vortices. In the orderly polarized vortex lattice, their dynamical properties can be represented by the dispersion curves and the density of states. These can be designed by choosing the combinations of vortex core polarizations. In this paper, we have used the rigid vortex model. This model is based on the assumption that vortices are rigid objects that do not deform as they move. However, in reality, when the vortex moves, the spin configuration around the disk edges changes to reduce stray fields. This discrepancy leads to overestimation of the eigenfrequency ω_0 and magnetostatic interaction energy between disks. Nevertheless we believe that this model is a good approximation and useful for qualitative understanding although we need to take into account non-nearest-neighbor disks in the case of large vortex displacement. Therefore, a more precise investigation on the dynamics of magnetic vortices needs to be carried out in future.

From our analysis, we can speculate on the following phenomena. A *randomly polarized vortex lattice* should reveal the localization behavior in the rotational motion of vortices in the real space as a consequence of various superposition of ferromagnetic type I and antiferromagnetic type II domains. In analogy with the lattice vibration of a coupled diatomic lattice, a *vortex lattice with two kinds of disks* is expected to exhibit an eigenfrequency gap in the dispersion curves. Furthermore the localization mode can be controlled since we can design a *defective lattice*. Finally, extension of the expected results encourages us to fabricate an electromagnetic waveguide in the artificial crystal of the magnetic vortex system similar to the two-dimensional photonic crystal.[19,20]

[1] T. Shinjo *et al.*, Science **289**, 930 (2000).
[2] A. Wachowiak *et al.*, Science **298**, 577 (2002).
[3] A. Hubert and R. Schäfer, *Magnetic Domains* (Springer, Berlin, 1998), p. 264.
[4] A. Aharoni, J. Appl. Phys. **68**, 2892 (1990).
[5] N. A. Usov and S. E. Peschany, J. Magn. Magn. Mater. **118**, L290 (1993).
[6] C. Miramond *et al.*, J. Magn. Magn. Mater. **165**, 500 (1997).
[7] R. P. Cowburn *et al.*, Phys. Rev. Lett. **83**, 1042 (1999).
[8] A. Fernandez and C. C. Cerjan, J. Appl. Phys. **87**, 1395 (2000).
[9] J. Raabe *et al.*, J. Appl. Phys. **88**, 4437 (2000).
[10] M. Schneider *et al.*, Appl. Phys. Lett. **77**, 2909 (2000).
[11] T. Okuno *et al.*, J. Magn. Magn. Mater. **240**, 1 (2002).
[12] K. Yu. Guslienko *et al.*, J. Appl. Phys. **91**, 8037 (2002).
[13] N. A. Usov and L. G. Kurkina, J. Magn. Magn. Mater. **242-245**, 1005 (2002).
[14] J. P. Park *et al.*, Phys. Rev. B **67**, 020403 (2003).
[15] J. Shibata *et al.*, Phys. Rev. B **67**, 224404 (2003).
[16] K. Yu. Guslienko *et al.*, Appl. Phys. Lett. **78**, 3848 (2001); Phys. Rev. B **65**, 024414 (2002).
[17] A. A. Thiele, Phys. Rev. Lett. **30**, 230 (1973).
[18] D. L. Huber, Phys. Rev. B **26**, 3758 (1982).
[19] S. Noda *et al.*, Science **289**, 604 (2000).
[20] S. Noda *et al.*, Science **293**, 1123 (2001).